Oil Shale, 2022, Vol. 39, No. 3, pp. 217–240
doi: https://doi.org/10.3176/oil.2022.3.04

Thermal methods of solid fuel processing: review

Zhannur Kadenovna Myltykbayeva, Zhaniya Turlykhanovna Yeshova, Madi Bekezhanuly Smaiyl*

Al-Farabi Kazakh National University, Almaty, Kazakhstan

Received 27 April 2022, accepted 15 July 2022, available online 10 September 2022

Abstract. *A review of literature data on the processing of solid types of combustible fossils into liquid fuels and chemical products has been carried out. The reserves of solid fossil fuels far exceed the natural resources of oil and gas, so the development of methods for processing solid fossil fuels into chemical products and liquid fuels is an urgent task. The main methods of processing coal and oil shale (OS) are reduced to pyrolysis and supercritical gasification. Pyrolysis is preferred for processing oil shale into shale oil, and currently a promising method for processing coal is extraction with supercritical solvents such as water and CO_2 at temperatures up to 900 °C and in some cases with the addition of a catalyst. For oil shale, the gasification process, like pyrolysis, is carried out under milder conditions, since the mineral part of oil shale contains trace elements that act as catalysts, and the structure of the organic part of oil shale is more similar in composition to oil.*

Keywords: *solid combustible minerals, oil shale, coal, pyrolysis, extraction, supercritical water, solvent extraction.*

1. Introduction

For billions of years, nature has accumulated in the earth's crust the richest reserves of carbon in the form of coal and brown coal, oil, gas, and oil shale (OS). Since the production of oil and gas as the main energy resources increases, their reserves decrease every year, whereas the existing reserves of solid fuels, unlike oil, can be used for several hundred years. In this regard, the processing of solid fossil fuels into chemical products and liquid fuels is currently an urgent task.

* Corresponding author: e-mail *oilcoal@mail.ru*

Of the available types of solid fuels, coal and shale are most suitable for liquefaction processes, but not all coals in different stages of coalification are fit for producing liquid products, the yield of which depends on the amount of volatile substances in coal. Coals in the lignite and sub-bituminous coal stages have the largest amount of volatile substances, and the yield of liquid products from stony and anthracite coals is very low, since carbon is firmly bound to the structures of macromolecules. Coals suitable for liquefaction account for about 30% of the total coal reserve in the world (1,069,636 million tons) [1].

Oil shale represents one of the potential sources of liquid fuel of the near future, its reserves are estimated at 6.05 trillion barrels of oil equivalent [2], while the proven volume of oil is only 1733.9 million barrels [1]. In terms of the composition of the organic mass, oil shale is more similar to oil than to coal. Kerogens from oil shales have a relatively high atomic ratio of hydrogen to carbon (usually 1.2–1.6), at least compared to coals, for which this ratio is usually less than one. It is the high ratio of hydrogen to carbon that makes kerogen from oil shales interesting as a potential source of liquid fuel. This is clearly seen in the molecular models of coal and oil shale (Fig. 1). Described by J. Shinn [3] (Fig.1a), the molecular model of coal mainly consists of condensed aromatic rings, whereas the model of the kukersite oil shale from Estonia (Fig. 1b) consists mainly of aliphatic structures [4].

In 2019, according to Looney [1], coal accounted for 53.87% of primary energy consumption in Kazakhstan, oil for 22.25%, natural gas for 20.64%, hydropower for 2.9% and renewable energy for 0.32%. There are over 300 known deposits of fossil coal in Kazakhstan, with geological reserves of 25.605 billion tons [1]. More than 90% of all coal reserves are concentrated in the central and northern parts of the country. The largest basins are Ekibastuz (11 billion tons), Karaganda (9 billion tons) and Turgay (5 billion tons). Coal exports account for about 1% of Kazakhstan's total exports.

(a)

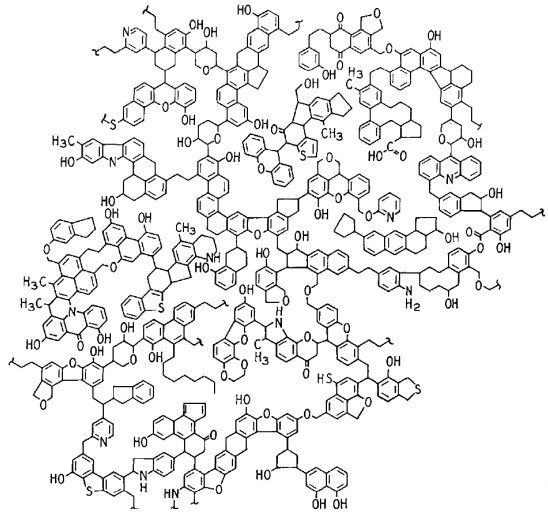

(b)

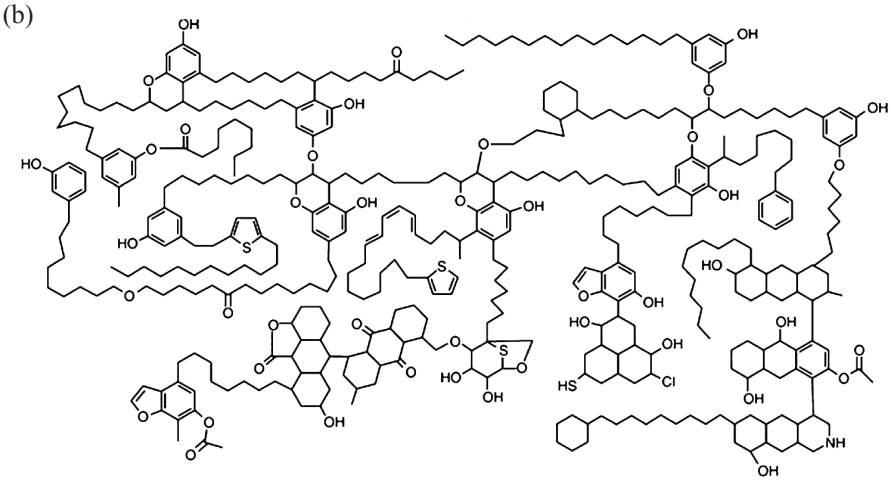

Fig. 1. Molecular model of coal (a) [3] and oil shale (b) [4].

There are also several oil shale deposits on the territory of Kazakhstan, the largest of them is the Kenderlyk coal-shale deposit (more than 6 billion tons) in the Zaisan depression, which is of practical interest both in terms of oil shale reserves and their quality. The main world reserves of oil shale are concentrated in the United States and amount to approximately 6 trillion barrels. Estonia, with a reserve of 16 billion barrels, is one of the main producers of shale oil in the amount of 1173 thousand tons per year (t.t./y.) [5], together with China's 1748 t.t./y. (approximately 35,000 barrels per day) [6, 7] and Brazil's 159 t.m.t. [2].

Coal has been mined and used as an energy source for centuries. The first recorded use of coal was in China, where it was employed for heating and metallurgy about 2500 years ago [8]. The first attempts to process oil shale date back to the beginning of the 19th century with the production of only a small amount of hydrocarbon raw materials [9].

Until the beginning of the 20th century, coal was the main energy source, but with the development of oil refining, it lost importance as the main raw material for the production of motor fuels. With the depletion of oil reserves, the problem of finding alternative sources of motor fuels becomes more urgent.

The first works on the production of synthetic liquid fuels from coal were carried out in 1913 by Friedrich Bergius in Germany [10]. Bergius treated crushed bituminous coal with hydrogen at high temperature and pressure in order to obtain a liquid product consisting of heavy oils, medium distillates, gasoline and gases. This method was later called hydrogenation. Afterwards, other methods of processing solid combustible minerals such as extraction (at boiling points and under critical conditions of solvents) and pyrolysis were also widely developed.

2. Pyrolysis of combustible minerals

Coal pyrolysis is mainly used in the metallurgical industry to produce coke, which is one of the key raw materials for the production of cast iron and steel. In pyrolysis processes, the H/C ratio in coal increases due to the removal of carbon. The coking process involves heating coal in closed containers to very high temperatures (up to 2000 °C) in the absence of oxygen. In such conditions, the molecular structure of coal is split into lighter substances with a lower molecular weight in a gaseous state. A solid porous residue remains, containing mainly carbon and inorganic ash. Synthesis gas and coal tar containing benzene, toluene, xylene, naphtha and ammonia are obtained from the by-products of high-temperature coking [11, 12].

For coal liquefaction, one of the main indicators is the yield of volatile substances, which is usually 5–30 wt% coal. The largest amount of volatile substances is formed by coals in the stage of lignite and subbituminous coal, which are the raw materials for liquefaction by pyrolysis. The pyrolysis of coal decomposes thermally unstable components and involves the release of low-molecular compounds, polycondensation of pyrolytic residues, decomposition and condensation of volatile products, and further formation of semi-coke or coke [13, 14]. Pyrolysis of coal is divided into two stages (Fig. 2). At the first stage (300 °C < 550 °C), primary pyrolysis (i.e. initial thermochemical reactions such as depolymerization of weak bridging bonds and polycondensation of aromatic rings) leads to the formation of primary volatile substances (gas) and non-volatile solid residues called semi-coke. Primary volatiles consist of light gases (for example, H_2, CO, CO_2, H_2O, CH_4 and other hydrocarbon gases) and heavy products called resins of composition C_6 and more. Semi-coke is obtained as a result of softening, swelling and sintering of coal particles. The second stage of pyrolysis (550 °C < 950 °C) is defined as secondary pyrolysis, including the release of secondary volatile substances and coke formed as a result of polycondensation and curing of the semi-coke formed at the first stage [15–17].

Low-temperature pyrolysis at a temperature of about 500 °C has historically been the most preferred thermochemical conversion process for high-quality oil shales. In this pyrolysis or retorting process, organic matter is converted into oil (shale oil), gas and solid residue (semi-coke). The pyrolysis process can be carried out by extracting oil shale and producing oil by heating it in ground installations, or by heating oil shale underground without extracting it and bringing it to the surface (underground retorting).

The processing of oil shale is mainly carried out by surface pyrolysis (retorting). To date, there are many methods of surface pyrolysis using different reactors. More than 20 methods of surface pyrolysis and more than 10 methods of underground pyrolysis have been described by Speight [19, 20]. Underground pyrolysis eliminates many of the problems associated with the extraction, processing and disposal of large amounts of waste that occur

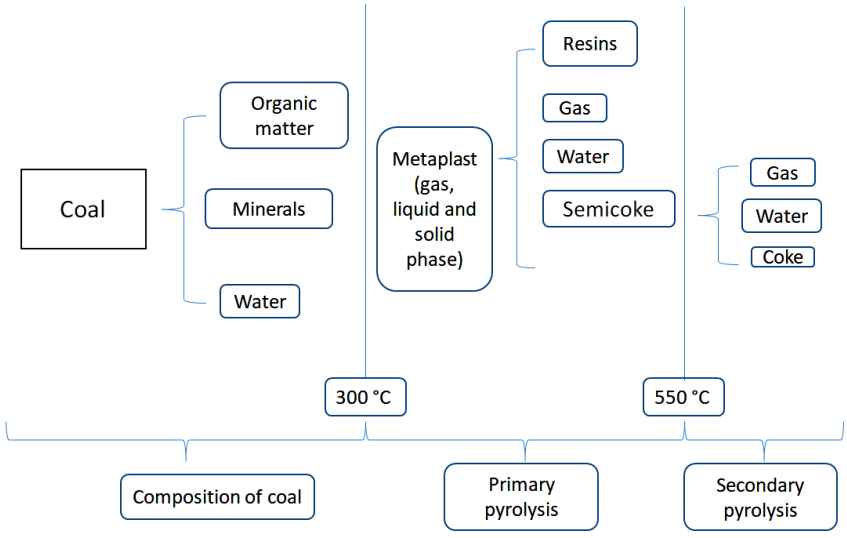

Fig. 2. Pyrolysis of coal [18].

during surface pyrolysis. Also, underground pyrolysis opens up opportunities for the extraction of shale oil from oil shale of thin and deep occurrence [20]. Currently, only four technologies are in commercial use, these are Kiviter, Galoter, Fushun and Petrosix [21].

Trace amounts of metals are contained in the oil shales of the Fushun, Maoming, Green River and Estonian deposits [22]. These elements act as catalysts in the pyrolysis of oil shales, enhancing pyrolytic reactions [23]. Korb et al. [24] used nuclear magnetic resonance (NMR) to study the organic structure and pore surface of minerals in oil shale in the presence of water, oil and gas and characterized the wettability of oil shale to investigate the possibility of on-site extraction of oil shale. The pyrolyzed compositions of organic substances were identified at 350–450 °C in Maoming oil shales, which included 272 inorganic compounds, 221 aromatic compounds and 81 alkanes and alkenes [25]. Shi et al. [26] demonstrated that the yield of shale oil from the Chinese Yaojie shale was about 85% during pyrolysis in the Sanjiang furnace at 550–700 °C, and the shale oil mainly consisted of diesel fuel and heavy components. The use of the NMR method to evaluate the properties of the kerogen and pyrolysis residues showed that the oil shale retorted in an open system at 500 °C contained larger aromatic clusters and more protonated aromatic fragments than in a closed system at 360 °C [27]. Alstadt et al. [28] compared the spectra of light and dark areas of oil shale samples and found the former areas to have a higher kerogen content, while the latter areas contained more mineral components (clay minerals, dolomite, calcite and pyrite).

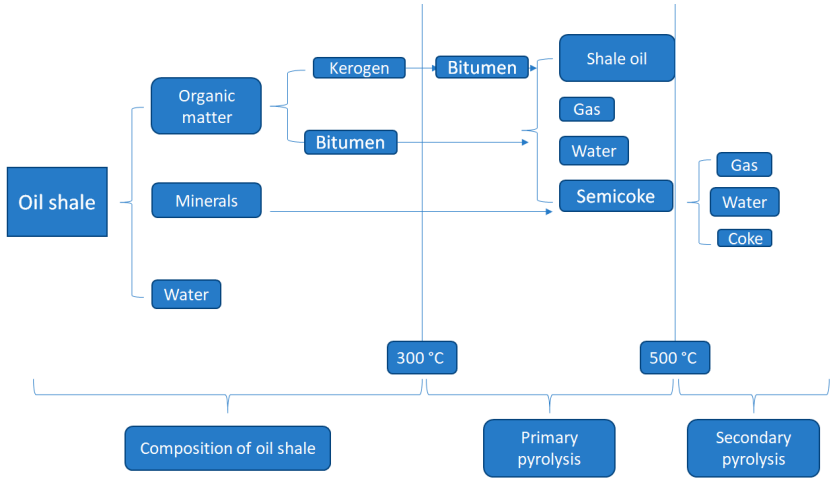

Fig. 3. Pyrolysis of oil shale [18].

During pyrolysis, the organic matter in oil shale decomposes, and volatile products are removed, while solid semi-coke or coke is formed [29, 30]. Essentially, pyrolysis of oil shale involves the decomposition of kerogen into bitumen, followed by decomposition into shale oil, gas, carbonaceous residues and pyrolytic water. It is important to note that carbon residues are mixed with minerals to form solid residues called semi-coke or coke [31–33]. In detail, the pyrolysis of OS can be mainly divided into two areas, as shown in Figure 3. The first region (300 °C < 500 °C) is the primary pyrolysis of kerogen with products in the form of oil, semi-coke, gas and water, the second region (500 °C < 900 °C) is the secondary pyrolysis of semi-coke formed in the primary pyrolysis region, which is processed into coke, gas and water [34–36].

Chinese scientists employed also another method of pyrolysis, in which oil shale was heated underground using superheated water vapor up to 500 °C [37]. 98% of China's oil shale reserves are unsuitable for surface processing processes [37]. Also, for many areas of oil shale occurrence in the Green River field of the USA, underground mining is more optimal. At the same time, for the open-pit extraction of oil shale, deposits with a thick layer are suitable, which make up 15% of the reserves of the Green River deposit [19]. Therefore, pyrolysis underground is considered the best option for processing oil shale for deposits in China and the United States. The following experimental conditions were used for pyrolysis of oil shale underground: wells for the transfer of coolant located every 50–200 m; fracturing of the oil shale formation along the fuel layers by hydraulic fracturing methods; the steam temperature of 500 °C, which provided sufficient heat for pyrolysis of kerogen. Kang et al. [38] obtained a 70.7% oil yield from the total volume of oil shale, and in the pyrolysis zone itself, the yield reached 95%.

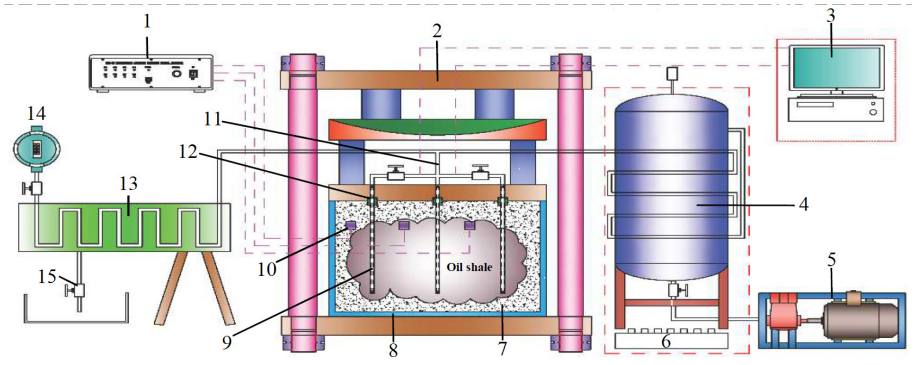

Fig. 4. Test system for pyrolysis of oil shale and extraction of oil and gas underground [38]: 1 – an acoustic emission system, 2 – a press machine with a capacity of 1000 tons, 3 – an automatic temperature and pressure control system, 4 – a heater, 5 – a water pump, 6 – a gas heater, 7 – concrete, 8 – the main chamber, 9 – wells, 10 – sample cracking detection systems, 11 – steam injection pipelines, 12 – seals, 13 – liquid cooling and separation systems, 14 – flow meter, 15 – liquid products output.

The pyrolysis process is still relevant for the production of shale oil from OS, as it is carried out at relatively low temperatures. Of the two types of pyrolysis of oil shale, pyrolysis underground is the most promising today, since it has such advantages as the absence of a large amount of residue and problems with the disposal of these wastes. Pyrolysis using heated water vapor as a coolant to produce shale oil underground is a promising processing method. The only disadvantage of this method is the long heating of the rock and heat removal after pyrolysis. Pyrolysis of coal is mainly used to produce coke, and the yield of liquid hydrocarbons is only a small part of the products obtained. Figure 4 shows the test system for pyrolysis of oil shale and extraction of oil and gas underground.

3. Solvent extraction

The solvent extraction process can be divided into two main types: solvent extraction at boiling points and solvent extraction under supercritical conditions.

3.1. Solvent extraction at boiling points

Extraction at boiling points of solvents has long been used to obtain valuable chemical products, in particular, rock wax from brown coals, lignites and peat. Coals of different types and stages of metamorphism swell at relatively

low temperatures, and a wide range of products can be extracted from them. Swelling is a consequence of the solvent "dissolving" in coal, and experimental data indicate that the process of coal swelling is reversible [39]. Numerous works of scientists show that much depends on the properties of the coal under study, such as the degree of metamorphism [40], the yield of volatile substances, and the petrographic component [41], as well as on the nature of the solvent that determines the temperature of the process [42]. It is at the boiling points of solvents that the greatest yield of products is observed. The yield of products is also influenced by the dimension of the solid fuel powder and the number of cycles of use of the condensed solvent. The solvents used can be divided into three groups:

1. neutral solvents, which include aliphatic hydrocarbons, aromatic hydrocarbons (benzene, toluene, naphthalene), oxygen-containing substances (ether, alcohol, ketone), chlorine-containing substances (chloroform, carbon tetrachloride), sulfur-containing substances (carbon disulphide);
2. mixed solvents, such as anthracene oil;
3. solvents of a basic nature, which include nitrogen-containing substances (of which pyridine, aniline and quinoline are the most studied) (Table 1).

Table 1. Extraction at boiling point of solvents

No	Solvent	Boiling point	Extraction yield	References
1	Benzene	80.1 °C	0.34–0.85% from oil shale 1–1.5% from brown coal	[43–45]
2	Hexane	68 °C	5–7% from brown coal	[46]
3	Chloroform	39.6 °C	1–9% from brown coal	[47]
4	Pyridine	115 °C	22–44% from brown coal	[48–50]
5	Tetrahydrofuran	66 °C	0.84–2.43% from oil shale, 8–14% from coal	[43, 45, 51]
6	Methylpyrrolidone	202 °C	43.9% from brown coal	[52]
7	Toluene	110.6 °C	1–2.06% from oil shale, 24–25% from coal	[53, 54]
8	Acetone	56 °C	0.55–1.16% from oil shale	[45]
9	Carbon disulfide	46.3 °C	0.28–1.09% from oil shale	[45]
10	Anthracene oil	340 °C	30–35% from coal	[55]
11	Carbazole	354.7 °C	19–45% from coal	[55]
12	Phenanthrene	340 °C	32–56% from coal	[55]
13	Morpholine	129 °C	23–33% from coal	[55]

Benzene extraction in the Soxlet apparatus gives a different bitumen yield for various combustible fossils. So, for peat from 8.0 to 22.5% and for brown coals, the yield of bitumen reaches 15%; benzene extracts about 0.5–1% of bitumen from hard coals [56]. Benzene extracts 1–1.5% of bitumen from brown coal deposits in the USA (Upper Freeport, Pittsburgh and Lewiston-Stockton) [44]. Fom the combustible shales of the Chang-7 deposit (China), when using benzene, the extract yield was 0.34–0.85% [43, 45]. Also, acetone, carbon disulfide and tetrahydrofuran with yields of 0.55–1.16%, 0.28–1.09% and 0.84–2.43%, respectively, were extracted from the oil shales of the Chang-7 deposit (China) using solvents. Tetrahydrofuran extracts 8–14% of the organic mass from Pingdingshan bituminous coal (China) (Table 1) [51].

The alcohol-benzene mixture makes it possible to isolate from brown coals from 2 to 20% of the organic mass, for hard coals this value reaches 3%, decreasing to 0% with an increase in the degree of carburization [56]. Toluene extracts 1–2.06% of the organic mass from the New Albany oil shale (USA), and 24–25% of bitumen was extracted from Recklinghausen coal (Germany), in which more than 20 polycyclic aromatic compounds were found [53, 54].

Hexane with a relatively low boiling point extracts bitumen from brown coal in the range of 5–7% [46].When extracting lignite coals from Bulgaria, Serbia, Poland and the Czech Republic, 1–9% of lipids from the total mass of coals were isolated by chloroform, which, according to infrared (IR) spectroscopy, are predominantly aliphatic in nature [47].

When pyridine is extracted, 10 to 20% of substances is extracted from fatty coals [56]. 22 to 44% of organic compounds pyridine is extracted from various brown coals [48–50]. Aniline extracts 26.8% of organic substances from fatty gas coal. As the degree of carburization increases, the yield of extracted substances decreases – the yield from bold coal is 7.2%, and aniline extracts only 1.8% from lean coal [56].

The amount of extracted substances also directly depends on the boiling point of the solvent, since with its increase, not only dissolution occurs, but also the destruction of intermolecular bonds [52, 55]. Methylpyrrolidone with a boiling point of 202 °C extracts 43.9% of the organic mass from brown coal and lignite deposits in Turkey [51].

Anthracene oil, carbazole and phenanthrene, with boiling points in the range of 340–350 °C, were extracted from Indian coals at 30–35%, 19–45% and 32–56% of organic mass, respectively [55]. Substances extracted by other neutral solvents having a higher boiling point than benzene or an alcohol-benzene mixture are not bitumen. Benzene dissolves only 30–50% of all substances extracted with pyridine, and the bulk of organic substances consists of alkanes (paraffins) C_{13}–C_{40}.

These data indicate that the organic mass of oil shale (kerogen), unlike that of coal, is more stable towards the effects of organic solvents, and the use of the extraction process is not considered effective in the case of kerogen. In contrast, up to 60% of organic substances can be extracted from low-grade

metamorphism coals at boiling points of solvents. The yield of the extract when using the same solvent for different coals may differ greatly, and this may be due to the nature and chemical properties of coals. In addition to the extract output, there are problems associated with the harmfulness of solvents [57]. For example, of polar solvents, only acetonitrile is partially approved for use as a solvent. At the same time, all hydrocarbons are harmful, but their harmfulness decreases with the addition of the CH_3 group as follows: benzene → toluene → xylene. All alcohols and ketones are recommended for use as a solvent, but they have not found application in extraction from coal and oil shale [58].

3.2. Solvent extraction under supercritical conditions

Solvent extraction under supercritical conditions is one of the most promising methods for obtaining products from solid combustible minerals. This is due to the fact that many solvents under supercritical conditions exhibit properties that are unattainable under normal conditions, for example, superfluidity, low viscosity and lack of surface tension (Fig. 5). Supercritical extraction has a number of significant advantages over organic solvent extraction: the extract does not need to be cleaned from the solvent (environmental friendliness of the process); in some cases, extraction can be selective by controlling the density of the solvent.

Table 2. Critical parameters of various solvents

Solvent	Critical temperature, T_{crit}	Critical pressure, P_{crit}	Critical density, ρ_{crit}
	K	MPa (atm)	g/cm^3
Carbon dioxide	303.9	7.38 (72.8)	0.468
Water	647.096	22.064 (217.755)	0.322
Methane	190.4	4.60 (45.4)	0.162
Ethane	305.3	4.87 (48.1)	0.203
Propane	369.8	4.25 (41.9)	0.217
Ethylene	282.4	5.04 (49.7)	0.215
Propylene	364.9	4.60 (45.4)	0.232
Methanol	512.6	8.09 (79.8)	0.272
Ethanol	513.9	6.14 (60.6)	0.276

Table 2 (continued)

Solvent	Critical temperature, T_{crit}	Critical pressure, P_{crit}	Critical density, ρ_{crit}
	K	MPa (atm)	g/cm^3
Ammonia	405.3	11.35 (115.7)	0.322
Xenon	289.5	5.84 (58.4)	1.110
Benzene	425	3.75 (37)	0.302

Of the above-listed solvents (Table 2), water and CO_2 are the most interesting under critical and supercritical conditions, since the cost of these solvents is relatively low, and the critical conditions of CO_2 are relatively mild compared to other solvents. For CO_2, the critical point is T_C = 31.0 °C and P_C = 7.38 MPa, and the conditions above and below are supercritical and subcritical, respectively.

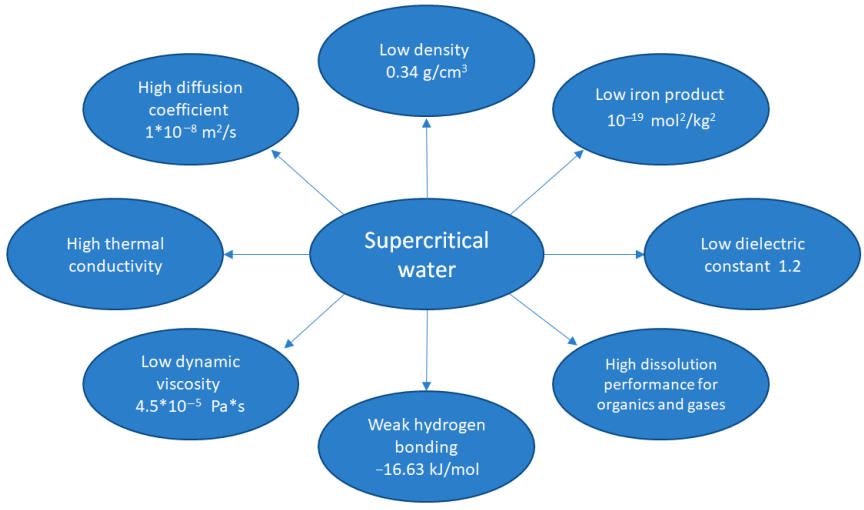

Fig. 5. Characteristics of supercritical water (SW) [59, 60].

Under supercritical conditions of water vapor and CO_2, the process takes place at the gasification stage and the main products are H_2, CO_2 and CH_4. When studying the possibility of processing coal and oil shale, water vapor has been mainly used in critical conditions recently.

3.2.1. Extraction from coal

Extraction under supercritical conditions of solvents is a multiparameter process, which is influenced by the following parameters: temperature, pressure, liquid:raw materials ratio, addition of oxidizer, and catalyst. Chen et al. [61] provided an overview of data on parameters affecting the process of supercritical coal extraction by water. The main data from this review are presented below.

The effect of temperature on supercritical gasification with water. Temperature is one of the most important factors for supercritical water gasification (SWG) technology [62–65]. When the temperature reaches the level of 800–950 °C, the efficiency of coal gasification (ECG) approaches 100%, while the proportion of hydrogen in the products reaches 60% and the proportion of methane decreases [62, 66, 67].

The effect of pressure on supercritical water gasification. The effect of pressure on the characteristics of the process is complex. Li et al. [62] noticed that the change in the efficiency of gasification with the formation of H_2, CO_2, and CH_4 fractions was small with a change in pressure. Jin et al. [66] showed that the peak of the H_2 fraction was observed at 25 MPa, and with increasing pressure, the characteristics of gasification changed little. Similarly, in an experiment on supercritical coal gasification with water conducted by Wang et al. [68] it was also found that pressure had little effect on gasification efficiency and gas composition. The mechanisms of pressure influence on gasification characteristics are very complex. In the SWG reaction itself, the reaction takes place in two stages: the first is the ionic reaction stage and the second is the free radical reaction. The ion reaction is facilitated under high pressure, but high pressure also has a positive effect on the gasification of SWG [69]. For example, high pressure leads to an increase in the density of supercritical water and ion reaction products. Therefore, hydrolysis reactions and extraction of volatile components from coal and pyrolysis reactions proceed under high pressure.

The effect of reaction time on supercritical water gasification. At the average temperature of the process, it takes a long time to establish the equilibrium of the reaction. As a rule, an increase in reaction time can increase the overall ECG. Lan et al. [70] indicated that the ECG increased from 24.24% to 42.36%, and the gasification efficiency (GE) increased from 50.05% to 93.09% when the reaction time increased from 4 min to 15 min. The molar fraction of H_2 increased from 39.83% to 45.53% when the reaction time increased from 4 min to 10 min. Jin et al. [71] discovered that the ECG increased from 33.89% to 37.96%, and the H_2 yield increased from 11.53 mol/kg to 14.92 mol/kg with increasing reaction time. Meanwhile, the ECG was found to increase significantly with time increasing for 1 minute, but the tendency of the ECG to increase weakened when the time increased from 1 minute to 2.3 minutes [67]. However, Jin et al. [71] indicated that the ECG increased only slightly when the reaction time had tripled. The ECG first increased and then decreased with

increasing flow, and the same change in hydrogen yield was also observed. The reason was that a higher flow rate led to a stronger heat and mass transfer in a continuous reactor [72]. Jin et al. [73] adopted a kinetic model for predicting the distribution of products in the SWG process.

Influence of the liquid:raw materials ratio for supercritical water gasification. The effect of coal concentration on coal SWG is significant. A higher concentration means a greater processing capacity of the SWG process. However, many studies have shown that during the gasification of raw materials with a high concentration of coal, a large number of charring products are formed (carbon structure remaining after thermal processes or semi-coke) [74]. The efficiency of coal gasification decreases and the proportion of H_2 and the yield of H_2 decrease with an increase in the concentration of coal [67, 71, 74, 75]. The reasons for these phenomena are as follows: 1) the mass exchange between water and coal decreases and 2) the high concentration of coal facilitates the methanation reaction by increasing the proportion of CH_4 and CO and reducing the proportion of H_2 and CO_2.

The effect of an oxidant additive on supercritical gasification with water. Many researchers carried out partial oxidation of various model compounds in supercritical water (SW) and pointed out that the oxidation reaction in SW can significantly improve the characteristics of gasification and reduce the formation of charring (semi-coke) [67, 70, 76, 77]. When an oxidizer (oxygen and peroxide) is added to the SW, the carbon contained in the coal can be oxidized by gaseous products, which can also be oxidized. For example, hydrogen can be oxidized to water, and CO can be oxidized to CO_2. Thus, when an oxidizer is added, the efficiency of carbon gasification increases but the yield of combustible gas decreases.

The effect of the catalyst on supercritical water gasification. To improve the characteristics of gasification and reduce the reaction temperature for complete gasification, the process of catalytic combustion of coal was studied in detail [70, 78, 79]. The catalysts used for coal SWG can be both homogeneous and heterogeneous.

Homogeneous catalysts, which are used in the processes of supercritical coal gasification, are well soluble in water. Wang and Takarada [80] carried out the SWG of coal with a batch reactor and came to the conclusion that the extraction of volatile substances was accelerated and coal production was reduced by using $Ca(OH)_2$ as a catalyst. Li et al. [62] conducted a catalytic SWG of coal and found Raney-Ni to be inferior in its catalytic characteristics to K_2CO_3. Ge et al. [81] carried out the SWG of coal with the addition of various catalysts. The results showed that the yield of H_2 relative to the alkaline catalyst varied in the following order: $K_2CO_3 = KOH = NaOH > Na_2CO_3 > Ca(OH)_2$ [81], and NaOH and KOH had the best catalytic characteristics. The reason was that the melting points of NaOH and KOH were 318.4 °C and 361 °C, respectively. Thus, NaOH and KOH in the SWG are in a molten state, which can increase the rate of mass transfer between catalysts and coal. Without the addition of

a catalyst, carbon reacts with the H_2O gasification agent in the SWG to form CO, which will contribute to the water-gas shift reaction and the methanation reaction [82]. H_2O oxidizes Me_2O–C to form Me_2O_2–C and H_2, creating a cycle that allows such oxidation to continue [81].

Along with the catalysts in the form of alkali metals mentioned above, heterogeneous catalysts are often used to improve the characteristics of the SWG gasification process. Compared to catalysts based on alkali metal compounds, heterogeneous catalysts have many advantages, such as high activity and the lack of corrosion problems. It is proven that metal catalysts containing Cr, Co, Ni, Mo, W, Zn, Ru, and Rh improve gasification characteristics during the subcritical/supercritical gasification of water and inhibit the formation of charring [83]. Some studies have shown that Ru is the most active catalyst [84], and the C–C bond is effectively destroyed when using Ru [85]. In addition, the carriers of metal catalysts have a significant effect on the characteristics of gasification [86]. A proper catalyst carrier must have high recoverability and the ability to accumulate oxygen [87]. Yu et al. [88] conducted a series of experiments on the gasification of brown coal in SW with the production of hydrogen. The efficiency of gasification, gas yield and hydrogen production increased significantly when Ru deposited on CeO_2-ZrO_2 was used as a catalyst. Guan et al. [89] found that when using 0.5 kg/kg Ru/CeO_2 (5%), the efficiency of carbon gasification increased by about 90%, and the yield of gaseous substances increased from 60% to 150% with a significant acceleration of the hydrogenation reaction.

As already mentioned, heterogeneous catalysts are easily restored, but the activity of catalysts decreases after restoration [89]. The efficiency of carbon gasification is 83.5% and 60.7%, respectively, when using fresh and reused catalysts [88]. Reducing the surface area of the catalyst can also lead to a decrease in the activity of the catalyst. The implementation of the reuse of a heterogeneous catalyst under the condition of high gasification efficiency is an urgent problem that needs to be solved.

3.2.2. Extraction from oil shale

Supercritical water extraction is widely used for coals of different stages of metamorphism. Catalytic SWG is especially interesting, and supercritical extraction from oil shale, unlike coal, has been studied less. However, there is evidence of the influence of some process parameters on the extraction from oil shale.

Studies have been conducted on the catalytic effects of $FeCl_2$, $CoCl_2$, $NiCl_2$ and $ZnCl_2$ on the gasification of oil shale in a fixed bed reactor, and it has been shown that the use of $CoCl_2$ and $NiCl_2$ gives a good catalytic effect [90]. The addition of iron chlorides $FeCl_2$ and $FeCl_3$ in the form of solutions to the supercritical gasification process at a temperature of 350 °C and a time of

20–70 hours increases the yield of gaseous substances up to 58.5% and also reduces the time (40 hours) of maximum kerogen gasification by 43%, while the conversion reaches 97.3% ($FeCl_2$) and 95.4% ($FeCl_3$) [91, 92].

When the temperature of the oil shale SWG changed from 500 °C to 700 °C, the gas output was increased from 56.24 to 161.08 l/kg [93]. Nasyrova et al. [94] carried out extraction from oil shale at 320 °C and 374 °C, as a result, the gas yield increased from 39.63% to 48.24%. Lu et al. [95] performed pyrolysis and SWG from the oil shale of the Fushong deposit (China) at equal temperature limits to determine the kinetics of changes in the yield of products. At temperatures of 350 °C and above, the reduction in the mass of oil shale is higher at supercritical extraction, reaches a maximum at 450 °C and is 12.3%. In the graphs of the kinetics of changes in the yield of gas products (H_2, CO_2, CH_4, C_2H_4, C_3H_8, C_{4+}), at a temperature below 360 °C, 60% of gas products is CO_2, and at a temperature of 450 °C, the amount of hydrocarbon gases increases to 58%, while the total amount of H_2 and CO_2 decreases to 42%. An increase in the amount of hydrocarbon gases has a positive effect on the quality of the resulting product. 68.6% of the products was extracted by SWG from Moroccan Tarfaya oil shale at a temperature of 390 °C and an extraction time of 150 minutes [96]. Chham et al. [97] used different solvents and wastewater from the olive oil production plant under sub- and supercritical conditions. At 374 °C and 132 bar, they obtained a maximum yield of 26.16% from the Moroccan Timahdit oil shale. With sub- and supercritical extraction, when the temperature rises, the process turns into gasification. For example, from the Natih B formation (Oman) oil shale at 300 °C, the yield of liquid products was 11.7% and with an increase in temperature to 400 °C, the yield of liquid products decreased to 10.1% and that of gas increased from 19.6% to 66.34% [98].

With an increase in the extraction time from 75 to 350 hours, the amount of C_2–C_6 hydrocarbons increased from 1.5% to 3.5% [99]. The influence of time (0–12 hours) on the yield of products at 750 °C and 24 MPa was studied using the oil shale from the Bohai Bay Basin deposit. When the extraction time reached 8 hours, the H_2 content increased to 41.3%. Also, with an increase in the extraction time from 0 to 8 hours, the gas output increased from 136.1 to 257.4 l/kg [93]. Kang et al. [92] noted that with an increase in the extraction time from 20 to 90 hours, the extract yield increased from 9% to 18%. Yang et al. [100] established that with time increasing from 2.5 to 4 h, the H_2 content decreased from 87.6% to 62.6% and that of CO_2 increased from 0.81% to 33.15%

In addition to using water as a solvent, several studies have employed CO_2, aromatic solvents (such as benzene, toluene) and ethanol for extraction [96, 97, 101, 102]. CO_2 as a cheap solvent is very interesting in supercritical extraction, and the main efforts of researchers in recent years have been directed at studying the wettability effect of coal and oil shale. Evaluation of the influence of the parameters of the supercritical extraction process, such

as temperature, pressure and time, on the number of cracks and the volume of pores in the rock appearing during the process allows us to evaluate the possibilities of extracting shale oil from hard-to-reach shale formations [103–105].

In supercritical extraction, the conversion of organic mass is not as important as the composition of the resulting products. This is because when the conversion of extraction processes reaches 99%, the composition of gases mainly consists of CO_2. Also, in the case of different oil shales, the composition of the products obtained varies, and sometimes the process parameters affect the H_2 and CO_2 content differently. The extraction processes of oil shale and coal differ in temperature. For coal extraction, temperatures up to 900 °C are used, whereas for oil shale the range is 400–450 °C, which is two times lower. This is due to the structure of the organic mass in solid fuels, in oil shale this mass consists of lighter hydrocarbons.

4. Conclusions

This article reviews the literature in the field of solid fuel processing. The following main conclusions can be drawn from this review:

1. In determining the possibilities of using solid combustible fossils to produce synthetic fuels, the structure of the organic mass and the H/C ratio play an important role. Oil shale in this direction is very important.
2. The most preferred process for processing oil shale is low-temperature pyrolysis at a temperature of about 500 °C. A more promising implementation of the pyrolysis process is heating oil shale underground using superheated water vapor as a heat source, with the output of shale oil and gas processing products to the surface. At the same time, trace elements that are part of the mineral part of the shale can act as catalysts.
3. Despite the fact that 60% of the extract yield is achieved by solvent extraction at boiling points from coals, the environmental friendliness of these solvents is under doubt. At the same time, ecological solvents give no significant results. In the case of oil shale, this method is completely ineffective.
4. When extracting oil shale with solvents under supercritical conditions (500–700 °C), high yields of mainly gaseous products (H_2, CO_2, CH_4) are obtained. Therefore, studies of such energy-consuming processes are less effective, differently from pyrolysis at 500 °C.
5. For the production of organic substances from coal, the most promising method is solvent extraction under critical conditions. In this direction, water and CO_2 are the most interesting solvents in critical and supercritical conditions with the addition of easily restored heterogeneous catalysts.

Acknowledgement

This work was supported by the Ministry of Education and Science of the Republic of Kazakhstan (Project no. ARP08856825-OT-20 of October 1, 2020 "Using vanadium porphyrinates extracted from Kazakhstan oils for catalytic processing of petroleum products").

REFERENCES

1. *Statistical Review of World Energy, 2020*, 69th edition. Bp, 1–66.
2. World Energy Council. *World Energy Resources, 2016.*
3. Shinn, J. H. From coal to single-stage and two-stage products: A reactive model of coal structure. *Fuel*, 1984, **63**(9), 1187–1196. doi:10.1016/0016-2361(84)90422-8
4. Lille, Ü., Heinmaa, I., Pehk, T. Molecular model of Estonian kukersite kerogen evaluated by ^{13}C MAS NMR spectra. *Fuel*, 2003, **82**(7), 799–804. doi:10.1016/s0016-2361(02)00358-7
5. *Estonian Oil Shale Industry Yearbook 2019* (Oone, A., Ed.), 2020, 1–66.
6. Li, S. The developments of Chinese oil shale activities. *Oil Shale*, 2012, **29**(2), 101–102.
7. Chen, A. *Petro China´s Gulong Shale Project May Bolster China´s Oil Output*. https://www.reuters.com/business/energy/petrochinas-gulong-shale-project-may-bolster-chinas-oil-output-2021-09-30/
8. Thomson, E. *The Chinese Coal Industry: An Economic History*. Routledge, London, 2002.
9. Dyni, J. R. *2004 Survey of Energy Resources. Oil Shale*, 2004, 73–91. doi:10.1016/b978-008044410-9/50007-3
10. Perry, H. Coal conversion technology. *Chem. Eng.*, 1974, **81**(15), 88–102.
11. White, L. C., Frederick, J. P. ENCOAL mild coal gasification project. In: *Proceedings of the 12th Annual International Pittsburgh Coal Conference*, Pittsburgh, PA, 11–15 Sep 1995, 151–156.
12. U.S. Department of Energy, National Energy Technology Laboratory. *The ENCOAL® Mild Coal Gasification Project. A DOE Assessment*. DOE/NETL-2002/1171.
13. Wu, J., Liu, Q., Wang, R., He, W., Shi, L., Guo, X., Chen, Z., Ji, L., Liu, Z. Coke formation during thermal reaction of tar from pyrolysis of a subbituminous coal. *Fuel Process. Technol.*, 2017, **155**, 68–73. doi:10.1016/j.fuproc.2016.03.022
14. Solomon, P. R., Serio, M. A., Suuberg, E. M. Coal pyrolysis: Experiments, kinetic rates and mechanisms. *Prog. Energy Combust. Sci.*, 1992, **18**(2), 133–220. doi:10.1016/0360-1285(92)90021-r
15. Geng, C., Li, S., Yue, C., Ma, Y. Pyrolysis characteristics of bituminous coal. *J. Energy Inst.*, 2016, **89**(4), 725–730. doi:10.1016/j.joei.2015.04.004
16. Lei, Z., Yang, D., Zhang, Y.-H., Cui, P. Constructions of coal and char molecular models based on the molecular simulation technology. *J. Fuel Chem. Technol.*, 2017, **45**(7), 769–779. doi:10.1016/S1872.5813(17)30038-5

17. Solomon, P. R., Fletcher, T. H., Pugmire, R. J. Progress in coal pyrolysis. *Fuel*, 1993, **72**(5), 587–597. doi:10.1016/0016-2361(93)90570-r
18. Liu, X., Cui, P., Ling, Q., Zhao, Z., Xie, R. A review on co-pyrolysis of coal and oil shale to produce coke. *Front. Chem. Sci. Eng.*, 2020, **14**(4), 504–512. doi:10.1007/s11705-019-1850-z
19. Speight, J. G. Mining and retorting. *Shale Oil and Gas Production Processes*. Gulf Professional Publishing, 2019, 797–847. doi:10.1016/b978-0-12-813315-6.00014-2
20. Speight, J. In situ retorting. *Shale Oil and Gas Production Processes*. Gulf Professional Publishing, 2019, 849–871. doi:10.1016/b978-0-12-813315-6.00015-4
21. Qian, J., Wang, J. World oil shale retorting technologies. In: *Int. Conf. on Oil Shale: Recent Trends in Oil Shale,* 7–9 November 2006, Amman, Jordan, 7–9.
22. Qian, J. L., Yin, L., Wang, J., Li, S., Han, F., He, Y. *Oil shale – Supplementary Energy of Petroleum*. Beijing: China Petrochemical Press, 2011.
23. Zheng, D., Li, S., Ma, G., Wang, H. Autoclave pyrolysis experiments of Chinese Liushuhe oil shale to simulate in-situ underground thermal conversion. *Oil Shale*, 2012, **29**(2), 103–114. doi:10.3176/oil.2012.2.02
24. Korb, J.-P., Nicot, B., Louis-Joseph, A., Bubici, S., Ferrante, G. Dynamics and wettability of oil and water in oil shales. *J. Phys. Chem.* C, 2014, **118**(40), 23212–23218. doi:10.1021/jp508659e
25. Guo, S., Ruan, Z. The composition of Fushun and Maoming shale oils. *Fuel*, 1995, **74**(11), 1719–1721. doi:10.1016/0016-2361(95)00137-t
26. Shi, Y., Li, S., Ma, Y., Yue, C., Shang, W., Hu, H., He, J. Pyrolysis of Yaojie oil shale in a Sanjiang-type pilot-scale retort. *Oil Shale*, 2012, **29**(4), 368–375. doi:10.3176/oil.2012.4.07
27. Cao, X., Birdwell, J. E., Chappell, M. A., Li, Y., Pignatello, J. J., Mao, J. Characterization of oil shale, isolated kerogen, and postpyrolysis residues using advanced 13C solid-state nuclear magnetic resonance spectroscopy. *AAPG Bull*., 2013, **97**(3), 421–436. doi:10.1306/09101211189
28. Alstadt, K. N., Katti, D. R., Katti, K. S. An *in situ* FTIR step-scan photoacoustic investigation of kerogen and minerals in oil shale. *Spectrochim. Acta A*, 2012, **89**, 105–113. doi:10.1016/j.saa.2011.10.078
29. Ma, Y., Li, S. The mechanism and kinetics of oil shale pyrolysis in the presence of water. *Carbon Resour. Convers.*, 2018, **1**(2), 160–164. https://doi.org/10.1016/j.crcon.2018.04.003
30. Qian, J., Wang, J., Li, S. World oil shale. *Energy of China*, 2006, **28**(8), 16–19 (in Chinese).
31. Külaots, I., Goldfarb, J. L., Suuberg, E. M. Characterization of Chinese, American and Estonian oil shale semicokes and their sorptive potential. *Fuel*, 2010, **89**(11), 3300–3306. https://doi.org/10.1016/j.fuel.2010.05.025
32. Han, X., Kulaots, I., Jiang, X., Suuberg, E. M. Review of oil shale semicoke and its combustion utilization. *Fuel*, 2014, **126**, 143–161. https://doi.org/10.1016/j.fuel.2014.02.045

33. Allred, V. D. Shale oil developments: Kinetics of oil shale pyrolysis. *Chem. Eng. Prog.*, 1966, **62**(8), 50–60.
34. Campbell, J. H., Gallegos, G., Gregg, M. Gas evolution during oil shale pyrolysis. 2. Kinetic and stoichiometric analysis. *Fuel*, 1980, **59**(10), 727–732. https://doi.org/10.1016/0016-2361(80)90028-9
35. Campbell, J. H., Koskinas, G. J., Gallegos, G., Gregg, M. Gas evolution during oil shale pyrolysis. 1. Nonisothermal rate measurements. *Fuel*, 1980, **59**(10), 718–726. https://doi.org/10.1016/0016-2361(80)90027-7
36. Yen, T. F., Chilingarian, G. V. *Oil Shale. Developments in Petroleum Science, 5*. Amsterdam: Elsevier, 1976.
37. Kang, Z., Zhao, Y., Yang, D. Review of oil shale in-situ conversion technology. *Appl. Energy*, 2020, **269**, 115121. doi:10.1016/j.apenergy.2020.115121
38. Kang, Z., Zhao, Y., Yang, D., Tian, L., Li, X. A pilot investigation of pyrolysis from oil and gas extraction from oil shale by *in-situ* superheated steam injection. *J. Petrol. Sci. Eng.*, 2020, **186**, 106785. doi:10.1016/j.petrol.2019.106785
39. Gyulmaliev, A. M., Golovin, G. S., Gladun, T. G. *Theoretical Foundations of Coal Chemistry*. – Moscow: Publishing House of the Moscow State Mining University, 2003 (in Russian).
40. Ulanovskii, M. L. Chemical aspects of coal metamorphism and the formation of low-molecular volatiles. *Coke and Chemistry*, 2012, **55**(12), 439–443. doi:10.3103/s1068364x1212006x
41. Epshtein, S. A., Suprunenko, O. I., Barabanova, O. V. The material composition and reactivity of vitrinites of hard coals of various degrees of reduction. *Solid Fuel Chemistry*, 2005, **39**(1), 19–31.
42. Makitra, R. G., Pristansky, Z. E. Dependence of the degree of swelling of coals on the physicochemical properties of solvents. *Solid Fuel Chemistry*, 2001, No. 5, 3–12 (in Russian).
43. Cao, Y., Han, H., Liu, H., Jia, J., Zhang, W., Liu, P., Ding, Z., Chen, S., Lu, J., Gao, Y. Influence of solvents on pore structure and methane adsorption capacity of lacustrine shales: An example from a Chang 7 shale sample in the Ordos Basin, China. *J. Petrol. Sci. Eng.*, 2019, **178**, 419–428. doi:10.1016/j.petrol.2019.03.052
44. Butala, S. J. M., Medina, J. C., Hulse, R. J., Bartholomew, C. H., Lee, M. L. Pressurized fluid extraction of coal. *Fuel*, 2000, **79**(13), 1657–1664. doi:10.1016/s0016-2361(00)00025-9
45. Cao, Y., Han, H., Guo, C., Pang, P., Ding, Z., Gao, Y. Influence of extractable organic matters on pore structure and its evolution of Chang 7 member shales in the Ordos Basin, China: Implications from extractions using various solvents. *J. Nat. Gas Sci. Eng.*, 2020, **79**, 103370. doi:10.1016/j.jngse.2020.103370
46. Liu, Y., Yan, L., Lv, P., Ren, L., Kong, J., Wang, J., Li, F., Bai, Y. Effect of n-hexane extraction on the formation of light aromatics from coal pyrolysis and catalytic upgrading. *J. Energy Inst.*, 2020, **93**(3), 1242–1249. doi:10.1016/j.joei.2019.11.007
47. Doskočil, L., Enev, V., Pekař, M., Wasserbauer, J. The spectrometric characterization of lipids extracted from lignite samples from various coal basins. *Org. Geochem.*, 2016, **95**, 34–40. doi:10.1016/j.orggeochem.2016.02.008

48. Niu, Z., Liu, G., Yin, H., Zhou, C., Wu, D., Yousaf, B., Wang, C. Effect of pyridine extraction on the pyrolysis of a perhydrous coal based on in-situ FTIR analysis. *J. Energy Inst.*, 2019, **92**(3), 428–437. doi:10.1016/j.joei.2018.05.005
49. Luo, A., Zhang, D., Zhu, P., Qu, X., Zhang, J.-L., Zhang, J.-S. Effect of pyridine extraction on the tar characteristics during pyrolysis of bituminous coal. *J. Fuel Chem. Technol.*, 2017, **45**(11), 1281–1288. doi:10.1016/s1872-5813(17)30058-0
50. He, Y., Zhao, R., Yan, L., Bai, Y., Li, F. The effect of low molecular weight compounds in coal on the formation of light aromatics during coal pyrolysis. *J. Anal. Appl. Pyrol.*, 2017, **123**, 49–55. doi:10.1016/j.jaap.2016.12.030
51. Zhang, S., Zhang, X., Hao, Z., Wang, Z., Lin, J., Liu, M. Dissolution behavior and chemical characteristics of low molecular weight compounds from tectonically deformed coal under tetrahydrofuran extraction. *Fuel*, 2019, **257**, 116030. doi:10.1016/j.fuel.2019.116030
52. Sönmez, Ö., Yıldız, Ö., Çakır, M. Ö., Gözmen, B., Giray, E. S. Influence of the addition of various ionic liquids on coal extraction with NMP. *Fuel*, 2018, **212**, 12–18. doi:10.1016/j.fuel.2017.10.017
53. Wei, L., Mastalerz, M., Schimmelmann, A., Chen, Y. Influence of Soxhlet-extractable bitumen and oil on porosity in thermally maturing organic-rich shales. *Int. J. Coal Geol.*, 2014, **132**, 38–50. doi:10.1016/j.coal.2014.08.003
54. Kerst, M., Andersson, J. T. Microwave-assisted extraction of polycyclic aromatic compounds from coal. *Fresenius J. Anal. Chem.*, 2001, **370**(7), 970–972. doi:10.1007/s002160100871
55. Sharma, D. K., Dhawan, H. Separative refining of coals through solvolytic extraction under milder conditions: A review. *Ind. Eng. Chem. Res.*, 2018, **57**(25), 8361–8380. doi:10.1021/acs.iecr.8b00345
56. Rapoport, I. B. *Artificial Liquid Fuel*. Moscow: Publishing House of Petroleum and Mining-Fuel Literature, 1955 (in Russian).
57. Prat, D., Pardigon, O., Flemming, H.-W., Letestu, S., Ducandas, V., Isnard, P., Guntrum, E., Senac, T., Ruisseau, S., Cruciani, P., Hosek, P. Sanofi's solvent selection guide: A step toward more sustainable processes. *Org. Process Res. Dev.*, 2013, **17**(12), 1517–1525. doi:10.1021/op4002565
58. Byrne, F. P., Jin, S., Paggiola, G., Petchey, T. H. M., Clark, J. H., Farmer, T. J., Hunt, A. J., McElroy, C. R., Sherwood, J. Tools and techniques for solvent selection: green solvent selection guides. *Sustain. Chem. Process.*, 2016, **4**(7). doi:10.1186/s40508-016-0051-z
59. Wei, N., Xu, D., Hao, B., Guo, S., Guo, Y., Wang, S. Chemical reactions of organic compounds in supercritical water gasification and oxidation. *Water Res.*, 2021, **190**, 116634. https://doi.org/10.1016/j.watres.2020.116634
60. Akizuki, M., Fujii, T., Hayashi, R., Oshima, Y. Effects of water on reactions for waste treatment, organic synthesis, and bio-refinery in sub- and supercritical water. *J. Biosci. Bioeng.*, 2014, **117**(1), 10–18. https://doi.org/10.1016/j.jbiosc.2013.06.011
61. Chen, J., Wang, Q., Xu, Z., E, J., Leng, E., Zhang, F., Liao, G. Process in supercritical water gasification of coal: A review of fundamentals, mechanisms, catalysts and element transformation. *Energy Convers. Manag.,* 2021, **237**, 114122. doi:10.1016/j.enconman.2021.114122

62. Li, Y., Guo, L., Zhang, X., Jin, H., Lu, Y. Hydrogen production from coal gasification in supercritical water with a continuous flowing system. *Int. J. Hydrog. Energy*, 2010, **35**(7), 3036–3045. https://doi.org/10.1016/j.ijhydene.2009.07.023
63. Yamaguchi, D., Sanderson, P. J., Lim, S., Aye, L. Supercritical water gasification of Victorian brown coal: Experimental characterisation. *Int. J. Hydrog. Energy*, 2009, **34**(8), 3342–3350. https://doi.org/10.1016/j.ijhydene.2009.02.026
64. Okolie, J. A., Rana, R., Nanda, S., Dalai, A. K., Kozinski, J. A. Supercritical water gasification of biomass: A state-of-the-art review of process parameters, reaction mechanisms and catalysis. *Sustain. Energy Fuels*, 2019, **3**(3), 578–598. https://doi.org/10.1039/C8SE00565F
65. Nanda, S., Isen, J., Dalai, A. K., Kozinski, J. A. Gasification of fruit wastes and agro-food residues in supercritical water. *Energy Convers. Manag.*, 2016, **110**, 296–306. https://doi.org/10.1016/j.enconman.2015.11.060
66. Jin, H., Lu, Y., Liao, Bo., Guo, L., Zhang, X. Hydrogen production by coal gasification in supercritical water with a fluidized bed reactor. *Int. J. Hydrog. Energy*, 2010, **35**(13), 7151–7160. https://doi.org/10.1016/j.ijhydene.2010.01.099
67. Ge, Z., Guo, S., Guo, L, Cao, C., Su, X., Jin, H. Hydrogen production by non-catalytic partial oxidation of coal in supercritical water: Explore the way to complete gasification of lignite and bituminous coal. *Int. J. Hydrog. Energy*, 2013, **38**(29), 12786–12794. https://doi.org/10.1016/j.ijhydene.2013.06.092
68. Wang, S., Guo, Y., Wang, L., Wang, Y., Xu, D., Ma, H. Supercritical water oxidation of coal: Investigation of operating parameters' effects, reaction kinetics and mechanism. *Fuel Process. Technol.*, 2011, **92**(3), 291–297. https://doi.org/10.1016/j. fuproc.2010.09.010
69. Adschiri, T., Sato, T., Shibuichi, H., Fang, Z., Okazaki, S., Arai, K. Extraction of Taiheiyo coal with supercritical water–HCOOH mixture. *Fuel*, 2000, **79**(3–4), 243–248. https://doi.org/10.1016/S0016-2361(99)00158-1
70. Lan, R., Jin, H., Guo, L., Ge, Z., Guo, S., Zhang, X. Hydrogen production by catalytic gasification of coal in supercritical water. *Energy Fuels* 2014, **28**(11), 6911–6917. https://doi.org/10.1021/ef502050p
71. Jin, H., Chen, Y., Ge, Z., Liu, S., Ren, C., Guo, L. Hydrogen production by Zhundong coal gasification in supercritical water. *Int. J. Hydrog. Energy*, 2015, **40**(46), 16096–16103. https://doi.org/10.1016/j.ijhydene.2015.09.003
72. Jin, H., Wang, Y., Wang, H., Wu, Z., Li, X. Influence of Stefan flow on the drag coefficient and heat transfer of a spherical particle in a supercritical water cross flow. *Phys. Fluids*, 2021, **33**(2), 023313. https://doi.org/10.1063/5.0041572.
73. Jin, H., Guo, L., Guo, J., Ge, Z., Cao, C., Lu, Y. Study on gasification kinetics of hydrogen production from lignite in supercritical water. *Int. J. Hydrog. Energy*, 2015, **40**(24), 7523–7529. https://doi.org/10.1016/j.ijhydene.2014.12.095
74. Jin, H., Zhao, X., Guo, S., Cao, C., Guo, L. Investigation on linear description of the char conversion for the process of supercritical water gasification of Yimin lignite. *Int. J. Hydrog. Energy*, 2016, **41**(36), 16070–16076. https://doi.org/10.1016/j.ijhydene.2016.05.129
75. Cao, C., Guo, L., Yin, J., Jin, H., Cao, W., Jia, Y., Yao, X. Supercritical water gasification of coal with waste black liquor as inexpensive additives. *Energy Fuels*, 2015, **29**(1), 384–391. https://doi.org/10.1021/ef502110d

76. Jin, H., Lu, Y., Guo, L., Cao, C., Zhang, X. Hydrogen production by partial oxidative gasification of biomass and its model compounds in supercritical water. *Int. J. Hydrog. Energy*, 2010, **35**(7), 3001–3010. https://doi.org/10.1016/j.ijhydene.2009.06.059
77. Muangrat, R., Onwudili, J. A., Williams, P. T. Reaction products from the subcritical water gasification of food wastes and glucose with NaOH and H_2O_2. *Bioresour. Technol.*, 2010, **101**(17), 6812–6821. https://doi.org/10.1016/j.biortech.2010.03.114
78. Kersten, S. R. A., Potic, B., Prins, W., Van Swaaij, W. P. M. Gasification of model compounds and wood in hot compressed water. *Ind. Eng. Chem. Res.*, 2006, **45**(12), 4169–4177. https://doi.org/10.1021/ie0509490
79. Lu, Y., Guo, L., Ji, C., Zhang, X., Hao, X., Yan, Q. Hydrogen production by biomass gasification in supercritical water: A parametric study. *Int. J. Hydrog. Energy*, 2006, **31**(7), 822–831. https://doi.org/10.1016/j.ijhydene.2005.08.011
80. Wang, J., Takarada, T. Role of calcium hydroxide in supercritical water gasification of low-rank coal. *Energy Fuels*, 2001, **15**(2), 356–362. https://doi.org/10.1021/ef000144z
81. Ge, Z., Jin, H., Guo, L. Hydrogen production by catalytic gasification of coal in supercritical water with alkaline catalysts: Explore the way to complete gasification of coal. *Int. J. Hydrog. Energy*, 2014, **39**(34), 19583–19592. https://doi.org/10.1016/j.ijhydene.2014.09.119
82. De Heer, J. The principle of Le Chatelier and Braun. *J. Chem. Educ.*, 1957, **34**(8), 375–380. https://doi.org/10.1021/ed034p375
83. Peterson, A. A., Vogel, F., Lachance, R. P., Fröling, M., Antal, Jr., M. J., Tester, J. W. Thermochemical biofuel production in hydrothermal media: A review of sub- and supercritical water technologies. *Energy Environ. Sci.*, 2008, **1**, 32–65. https://doi.org/10.1039/b810100k
84. Guan, Q., Mao, T., Zhang, Q., Miao, R., Ning, P., Gu, J., Tian, S., Chen, Q., Chai, X. Catalytic gasification of lignin with Ni/Al_2O_3–SiO_2 in sub/supercritical water. *J. Supercrit. Fluids*, 2014, **95**, 413–421. https://doi.org/10.1016/j.supflu.2014.10.015
85. Zhu, C., Guo, L., Jin, H., Huang, J., Li, S., Lian, X. Effects of reaction time and catalyst on gasification of glucose in supercritical water: Detailed reaction pathway and mechanisms. *Int. J. Hydrog. Energy*, 2016, **41**(16), 6630–6639. https://doi.org/10.1016/j.ijhydene.2016.03.035
86. Yamaguchi, A., Hiyoshi, N., Sato, O., Shirai, M. Gasification of organosolv-lignin over charcoal supported noble metal salt catalysts in supercritical water. *Top. Catal.*, 2012, **55**(11–13), 889–896. https://doi.org/10.1007/s11244-012-9857-4
87. Monte, M., Gamarra, D., López Cámara, A., Rasmussen, S. B., Gyorffy, N., Schay, Z., Martinez-Arias, A., Conesa, J. C. Preferential oxidation of CO in excess H_2 over CuO/CeO_2 catalysts: Performance as a function of the copper coverage and exposed face present in the CeO_2 support. *Catal. Today*, 2014, **229**, 104–113. https://doi.org/10.1016/j.cattod.2013.10.078

88. Yu, J., Lu, X., Shi, Y., Chen, Q., Guan, Q., Ning, P., Tian, S., Gu, J. Catalytic gasification of lignite in supercritical water with Ru/CeO_2–ZrO_2. *Int. J. Hydrog. Energy*, 2016, **41**(8), 4579–4591. https://doi.org/10.1016/j.ijhydene.2015.12.152
89. Guan, Q., Huang, X., Liu, J., Gu, J., Miao, R., Chen, Q., Ning, P. Supercritical water gasification of phenol using a Ru/CeO_2 catalyst. *Chem. Eng. J.*, 2016, **283**, 358–365. https://doi.org/10.1016/j.cej.2015.05.033
90. Chang, Z., Chu, M., Zhang, C., Bai, S., Ma, L. Investigation of the effect of selected transition metal salts on the pyrolysis of Huadian oil shale, China. *Oil Shale*, 2017, **34**(4), 354–367. doi:10.3176/oil.2017.4.04
91. Kang, S., Sun, Y., Deng, S., Li, S., Su, Y., Guo, W., Li, J. Extraction of Huadian oil shale in subcritical $FeCl_2$ solution. *Fuel Process. Technol.*, 2021, **211**, 106571. https://doi.org/10.1016/j.fuproc.2020.106571
92. Kang, S., Sun, Y., Qiao, M., Li, S., Deng, S., Guo, W., Li, J., He, W. The enhancement on oil shale extraction of $FeCl_3$ catalyst in subcritical water. *Energy*, 2022, **238**, Part A, 121763. doi:10.1016/j.energy.2021.121763
93. Liang, X., Zhao, Q., Dong, Y., Guo, L., Jin, Z., Liu, Q. Experimental investigation on supercritical water gasification of organic-rich shale with low maturity for syngas production. *Energy Fuels*, 2021, **35**(9), 7657–7665. doi:10.1021/acs.energyfuels.0c04140
94. Nasyrova, Z. R., Kayukova, G. P., Vakhin, A. V., Djimasbe, R., Chemodanov, A. E. Heavy oil hydrocarbons and kerogen destruction of carbonate–siliceous domanic shale rock in sub- and supercritical water. *Processes*, 2020, **8**(7), 800. doi:10.3390/pr8070800
95. Lu, Y., Wang, Z., Kang, Z., Li, W., Yang, D., Zhao, Y. Comparative study on the pyrolysis behavior and pyrolysate characteristics of Fushun oil shale during anhydrous pyrolysis and sub/supercritical water pyrolysis. *RSC Adv.*, 2022, **12**(26), 16329–16341. https://doi.org/10.1039/D2RA02282F
96. Abourriche, A., Oumam, M., Mansouri, S., Mouiya, M., Rakcho, Y., Benhammou, A., Abouliatim, Y., Alami, J., Hannache, H. Effect of processing conditions on the improvement of properties and recovering yield of Moroccan oil shale. *Oil Shale*, 2022, **39**(1), 61–78. doi:10.3176/oil.2022.1.04
97. Chham, A., Khouya, E., Abourriche, A. K., Oumam, M., Gmouh, S., Mansouri, S., El Harti, M., Hannache, H.. Supercritical water extraction and characterization of Moroccan shale oil by different solvent. *J. Mater. Environ. Sci.*, 2018, **9**(6), 1771–1778. https://doi.org/10.26872/jmes.2018.9.6.197
98. Saeed, S. A., Taura, U., Al-Wahaibi, Y., Al-Muntaser, A. A., Yuan, C., Varfolomeev, M. A., Al-Bahry, S., Joshi, S., Djimasbe, R., Suwaid, M. A., Kadyrov, R. I., Galeev, R, I., Naabi, A., Hasani, M., Al Busaidi, R. S. Hydrothermal conversion of oil shale: Synthetic oil generation and micro-scale pore structure change. *Fuel*, 2022, **312**, 122786. https://doi.org/10.1016/j.fuel.2021.122786
99. Sun, Y., Kang, S., Wang, S., He, L., Guo, W., Li, Q., Deng, S. Subcritical water extraction of Huadian oil shale at 300 °C. *Energy Fuels*, 2019, **33**(3), 2106–2114. doi:10.1021/acs.energyfuels.8b04431

100. Yang, D., Wang, L., Zhao, Y., Kang, Z. Investigating pilot test of oil shale pyrolysis and oil and gas upgrading by water vapor injection. *J. Petrol. Sci. Eng.*, 2021, **196**, 108101. https://doi.org/10.1016/j.petrol.2020.108101
101. Fomitšov, M. Low-temperature supercritical conversion of kukersite oil shale. *Oil Shale*, 2019, **36**(2S), 171–178. https://doi.org/10.3176/oil.2019.2S.07
102. Yang, T., Zhou, B., Li, R., Li, B., Zhang, W., Kai, X. Liquefaction of oil shale in supercritical ethanol. *Oil Shale*, 2018, **35**(3), 279–289. doi:10.3176/oil.2018.3.07
103. Zhang, G., Ranjith, P. G., Li, Z., Gao, M., Ma, Z. Long-term effects of CO_2-water-coal interactions on structural and mechanical changes of bituminous coal. *J. Petrol. Sci. Eng.*, 2021, **207**, 109093. doi:10.1016/j.petrol.2021.109093
104. Yu, H., Xu, H., Fu, W., Lu, X., Chen, Z., Qi, S., Wang, Y., Yang, W., Lu, J. Extraction of shale oil with supercritical CO_2: Effects of number of fractures and injection pressure. *Fuel*, 2021, **285**, 118977. doi:10.1016/j.fuel.2020.118977
105. Cheng, Y., Zhang, X., Lu, Z., Pan, Z. jun, Zeng, M., Du, X., Xiao, S. The effect of subcritical and supercritical CO_2 on the pore structure of bituminous coals. *J. Nat. Gas Sci. Eng.*, 2021, **94**, 104132. doi:10.1016/j.jngse.2021.104132